

A. CSAPAI^{1*}, D.-A. ȚOC², V. PAȘCALĂU¹, V. TOȘA¹, D. OPRUȚA³, F. POPA¹, C. POPA¹

STUDY ON THE EFFECT OF IN SITU SURFACE TREATMENTS OF MEDICAL MICROFLUIDIC SYSTEMS OBTAINED THROUGH ADDITIVE MANUFACTURING

This paper presents a comparative study on the effects of the in-situ surface modifications performed on “H” type microfluidic systems obtained via additive manufacturing. The microsystem was printed using a polylactic acid filament on an Ender-5 Pro printer. The surface modification of the main channel was done using chloroform by two different methods: vapor smoothing and flushing. The obtained surface roughness was studied using an optical microscope and the ImageJ software, as well as scanning electron microscopy. The effect of the channel surface treatment upon the characteristics of the fluid flow was assessed. The microfluidic systems were used for the dynamic study of biofilm growth of *Candida albicans* (ATCC 10231). The influence of the surface roughness of the main channel on the formation and growth of the biofilm was studied using quantitative methods, scanning electron microscopy imaging as well as optical coherence tomography.

Keywords: additive manufacturing; microfluidic systems; surface roughness; biofilm growth; laminar flow

1. Introduction

Microfluidics is an interdisciplinary science that addresses the concept of fluids being directly manipulated using microscale devices developed as a result of decades of advancements in the semiconductor industry and later on the growth and development of microelectromechanical systems (MEMS) [1]. With numerous advantages, such as the possibility of mathematical modelling of the laminar flow, the possibility of direct interaction with cells, increased surface to volume ratio, reduced production costs, and the possibility of automation and batch production [2], microfluidics is an ever evolving research field providing benefits to the chemical, biological and biomedical fields [3].

One of the fundamental goals of the microfluidics is to facilitate the development of technologies that assist and support the research within the biological and medical fields [1] by implementing and integrating different fluid manipulation components, analytical separation, and detection techniques on individual microfabricated devices [4].

Another significant question is directly related to the fabrication method of the microsystems. Throughout the years several fabrication techniques have been developed for the manufacturing of the microfluidic devices, which include wet

etching, reactive ion etching, machining, poly lithography, soft lithography, hot embossing, injection moulding, laser ablation, in situ construction, and plasma etching [4-9]. Recently, additive manufacturing (AM), a new fabrication technique that allows rapid device prototyping, has emerged [10]. AM is an assembly of widespread technologies used for the fabrication of polymer components from prototypes to functional structures [11]. 3D printing relies on the layer-by-layer fabrication method and allows building the model directly from a computer-aided design (CAD) drawing. A particular example of a 3D printing technique is the fused deposition modelling (FDM), which involves heating up a thermoplastic to a semi-liquid state and depositing it in ultra-fine beads along the extrusion path [12].

Numerous applications of the microfluidic devices have been based on poly-dimethyl siloxane (PDMS), due to its multiple advantages, such as non-toxicity, optical transparency, low surface energy and chemical inertness [13]. However, polylactic acid (PLA) has recently emerged as a more accessible and common material for 3D printing. It is derived from renewable resources, it is biodegradable, nontoxic, and inexpensive. The PLA monomer can be easily cured with good yield, high molecular weight, and can have amorphous or semicrystalline polymer characteristics [14].

¹ MATERIALS SCIENCE AND ENGINEERING DEPARTMENT, TECHNICAL UNIVERSITY OF CLUJ-NAPOCA, 103-105 MUNCII AVE., 400641 CLUJ-NAPOCA, ROMANIA

² IULIU HATIEGANU UNIVERSITY OF MEDICINE AND PHARMACY, 8 VICTOR BABEȘ STREET, 400000 CLUJ-NAPOCA, ROMANIA

³ THERMAL ENGINEERING DEPARTMENT, TECHNICAL UNIVERSITY OF CLUJ-NAPOCA, 103-105 MUNCII AVE., 400641 CLUJ-NAPOCA, ROMANIA

* Corresponding author: Alexandra.Csapai@stm.utcluj.ro



Biofilm science and technology has received much attention over the last four decades, after the first definition of biofilm was brought to public attention by Bill Costerton and co-workers in 1978 [15]. Biofilms are aggregations of microorganisms attached to and growing on a surface [16]. However, biofilms are much more than just a simple mass of attached microbial cells; they are intricate and structured microbial communities attached to a surface, to interfaces or to each other and are enclosed in a self-produced extracellular polymeric matrix [17,18]. By mimicking real environmental conditions of biofilm formation and growth through microfluidic devices, we can gain a better knowledge and understanding of the biofilms as a whole and at a single cell level, thus enabling control over deleterious biofilms, such as clinical biofilms, food contaminants, biofouling on industrial equipment and on ship hulls. The advantage of using microfluidic devices for studying the formation and growth of biofilms is that the devices provide a closed system which allows the interaction of the bacterial biofilm with hydrodynamic environments, enabling the development of mathematical models that account for these interactions and reveal the effects of several influencing factors on the formation of the biofilm [19].

Several measurement and characterization techniques are available for the assessment of biofilm formation and growth. The ultraviolet–visible spectroscopy (UV-VIS) allows the quantification of microbial organisms based on the fluorescence and wavelengths emitted by the cells when excited by UV or Visible light [20]. Scanning electron microscopy (SEM) facilitates the observation of the spatial structure of the biofilm, the effects of exposure to antibiofilm drugs, and allows the kinetics assessment [19]. Additionally, optical coherence tomography (OCT) can provide valuable information regarding the biofilm thickness and morphology by light scattering. Objects with higher light scattering will yield higher signal intensities than objects with lower scattering, thus allowing the visualization of different shades of white-black on the OCT images [21].

This paper aims to identify an efficient in-situ surface treatment procedure for PLA microfluidic devices obtained through additive manufacturing. Two different approaches were taken to obtain smooth channel surfaces for testing their interaction with suspensions of fungal colonies. The investigation focuses on the possible methods of in-situ surface treatment for microsystems obtained via additive manufacturing, as well as on the influence of the surface quality of the channel on the formation and growth of biofilms.

2. Materials and methods

2.1. The microfluidic system

In preparing the microfluidic device, a 1.75 mm, high performance PLA filament (Verbatim™) was used, as well as the Creality3D Ender 5 printer. The in-situ surface treatment of the central channel was done using Chloroform (CHCl₃), as an organic solvent, and a Werther Silent Air Compressor to

circulate the vapors in the microsystem. Additionally, to ensure the full enclosure and sealing of the microsystem, the Buildfix Pro DC hybrid composite was used for the UV soldering of the inlet/ outlet adapters. An SP230iwZ Syringe Pump (WPI) was used to circulate the fluids within the system. The study of biofilm formation and growth was done using a suspension of *Candida albicans* (ATCC 10231) at 4 McFarland turbidity, together with a nutrient broth (Thermo Scientific™, Nutrient Broth (Dehydrated), CM0001B). In preparing the fungi culture, a Sabouraud Agar medium was used.

The design of the H type microfluidic system was done using the SolidWorks 3D CAD Software. The model was printed on the Ender 5 printer, using the following settings: the nozzle temperature was set to 205°C, bed temperature was 60°C, layer height of 0.1 mm, infill of 80%, and print speed of 80 mm/s.

The in-situ surface treatment of the main channel was attempted with two different methods. The initial method implied the use of a custom-made vaporizer and a compressor, air pressure of 2 bar, to circulate the Chloroform vapors through the microchannels. This method of vapor smoothing was considered for the PLA parts, as it is reported in the literature as a common surface treatment procedure for PMMA and ABS FDM parts [22-25].

Another method used for the in-situ surface treatment involved flushing the microsystem with Chloroform. Two plastic tubes were attached to the inlets and outlets of the channel and using a syringe, 2.5 ml of Chloroform were pushed through the system. The following step was washing out the channels with 20 ml of water, making sure that all the Chloroform and plastic residues were removed. The obtained microsystems were characterized by optical microscopy, SEM and OCT.

2.2. Biofilm formation and growth

The *Candida albicans* (ATCC 10231) was cultivated on a Sabouraud Agar and incubated for 24 h at 37°C. The fungal suspensions were inoculated by picking up the colonies from the plate in a 10 ml Saline Solution, to obtain the 4McF turbidity. Plastic tubes were attached to the pipette heads on the inlets and outlets of the microfluidic devices to facilitate the circulation of the fluid within the system. Two syringes filled with the fungal suspension and nutrient broth, respectively, were connected to the plastic tubes. The suspensions ran through the microsystems with volumetric flow rates of 0.1 ml/min, 0.2 ml/min and 0.3 ml/min. The microsystems were held in an incubator at 37°C for 48 hours and inactivated by UV light.

2.3. Analysis methods

The quantitative analysis of biofilm formation was done using an adjusted microtiter plate technique adapted to this device. Initially, 5 ml of Saline Solution were used to wash out the planktonic cells. Subsequently, a 5 ml 1% crystal violet solution was used to stain the biofilm, followed by a 15-minute

incubation period at room temperature. Thirdly, 3 consecutive washes with Saline Salt were performed to ensure full removal of the excess dye. Lastly, 5 ml of ethanol with acetone were used to solubilize the stained biofilm. The obtained solution was diluted 1:10 with ethanol- acetone and assessed at 590 nm using a UV-Vis spectrometer.

The spectral domain optical coherence tomography (SD-OCT) measurements were recorded with an OPTH-1300 Handheld Scanner, central wavelength of 1300 nm, equipped with an OPTH-LK30 lens kit with a focal length of 30 mm, working distance of 22 mm, and field view of 10 mm, respectively, were used to establish the formation of biofilm in the microchannels. The lateral resolution is 24 μm , axial resolution of 5.5 μm in air, sensitivity of 76 kHz, refractive index of 1.90 mm, and pixel resolution of 1.85 $\mu\text{m}/\text{px}$.

The JEOL/JSM 5600-LV scanning electron microscope (SEM), with the accelerating voltage of 10 kV, and SEI signal was used to assess the topography of the surface of the biofilm within the channels. For both investigations, the microsystems were cut in four pieces through mechanical means, about 8 mm from the inlet and outlet channels and along the central channel. For SEM imaging, the samples were coated with Carbon, using a sputtering equipment, thus ensuring their electric conductivity.

The Brookfield DV2T Touch Screen Viscometer was used to perform the viscosity measurements of the 0.9% Saline Salt, as well as 3 dilutions of the *Candida* suspension: 4McF, 2McF and 1McF, respectively. The measurements were performed at room temperature, using the single point viscosity test method, the guard leg and the LV1 spindle, at 140-200 RPM, in a 600 ml container.

3. Results and discussions

The surface roughness of the central channel was analysed using an optical microscope, SEM images, OCT images, and the ImageJ software. Fig. 1a-c show the comparative images between the original microchannel, the vapor treated surface, and the in- situ smoothed channel. The first image shows the side wall of the channel previous to any surface treatment. Using the ImageJ software, the droplets of the PLA deposited filaments were measured along the wall. The obtained results vary between 113 μm droplet length and 120 μm droplet height for the untreated system and 146 μm droplet length and 41 μm droplet height for the Chloroform flushed microsystem. Fig. 2a and 2b present the OCT images of the original microsystem compared to the smoothed one. It may be noted that the outline of the droplets is well distinguishable in the first image, whereas in the second, the droplets are almost fully levelled. Both images were taken perpendicularly to the direction of the filament deposition during manufacturing.

The first SEM image (Fig. 3a) shows the display of the PLA filaments along the bottom of the channel; they appear parallel, about 100 μm away from each other. In contrast, the second SEM image (Fig. 3b) reveals the absence of these parallel filament lines, indicating a smooth surface. However, the second image also shows the presence of pores along the channel walls.

Fig. 4 shows the OCT images obtained along the filament deposition direction, for both the smoothed and untreated channels. Images 4a and 4b show the microsystems tested at a flow rate of 0.1 ml/min. Both reveal the formation of biofilm in a non-uniform layer, with a thickness of around 10 μm for the original

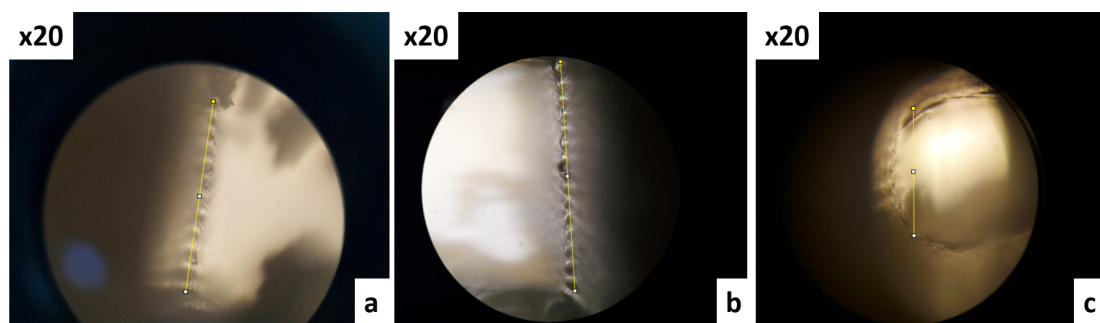


Fig. 1. Optical microscope ($\times 20$) images of the central channel of the a) Original microsystem; b) Vapor- treated microsystem; c) In- situ surface treated microsystem

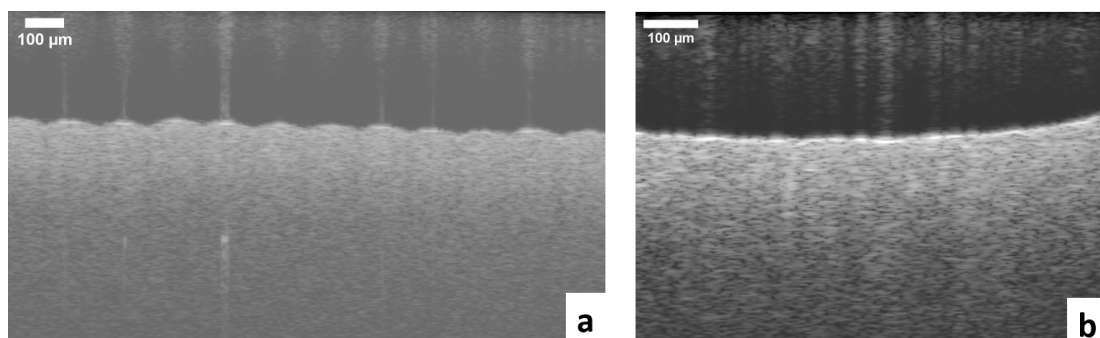


Fig. 2. OCT images of the central channel of the a) Original microsystem; b) In- situ surface treated microsystem

microsystem and about $9\ \mu\text{m}$ for the one with smoothed microchannels. Similarly, Fig. 4c-f show the untreated and smoothed microsystems tested at flow rates of 0.2 and 0.3 ml/min, respectively. For the untreated microchannels the biofilm thickness was around $7\ \mu\text{m}$ for the one tested at 0.2 ml/min and 6 for the one tested at 0.3 ml/min. In comparison for the equivalent smoothed channels, the biofilm thickness was around $6\ \mu\text{m}$ and $4\ \mu\text{m}$.

The SEM images (Figs. 5, 6 and 7) provide an overview of

the biofilm formation in the original microchannels compared to the smoothed microchannels, as well as the influence of the flow rate on the growth of the biofilm. The first four images show both the untreated and surface treated microsystems tested at 0.1 ml/min flow rate. Comparing the images, it can be observed that on the untreated surface the biofilm appears to be well attached to the walls, packed, possibly in multiple layers, whereas on the smooth surface there are much less colonies visible, with

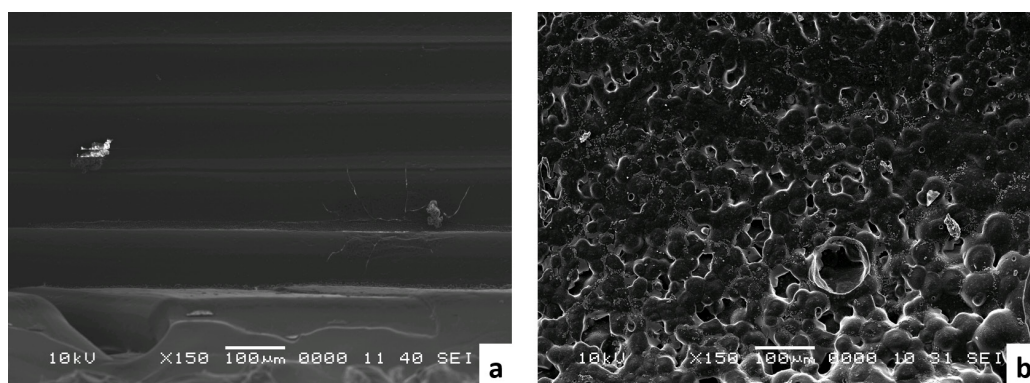


Fig. 3. SEM images of the central channel of the a) Original microsystem; b) In-situ surface treated microsystem

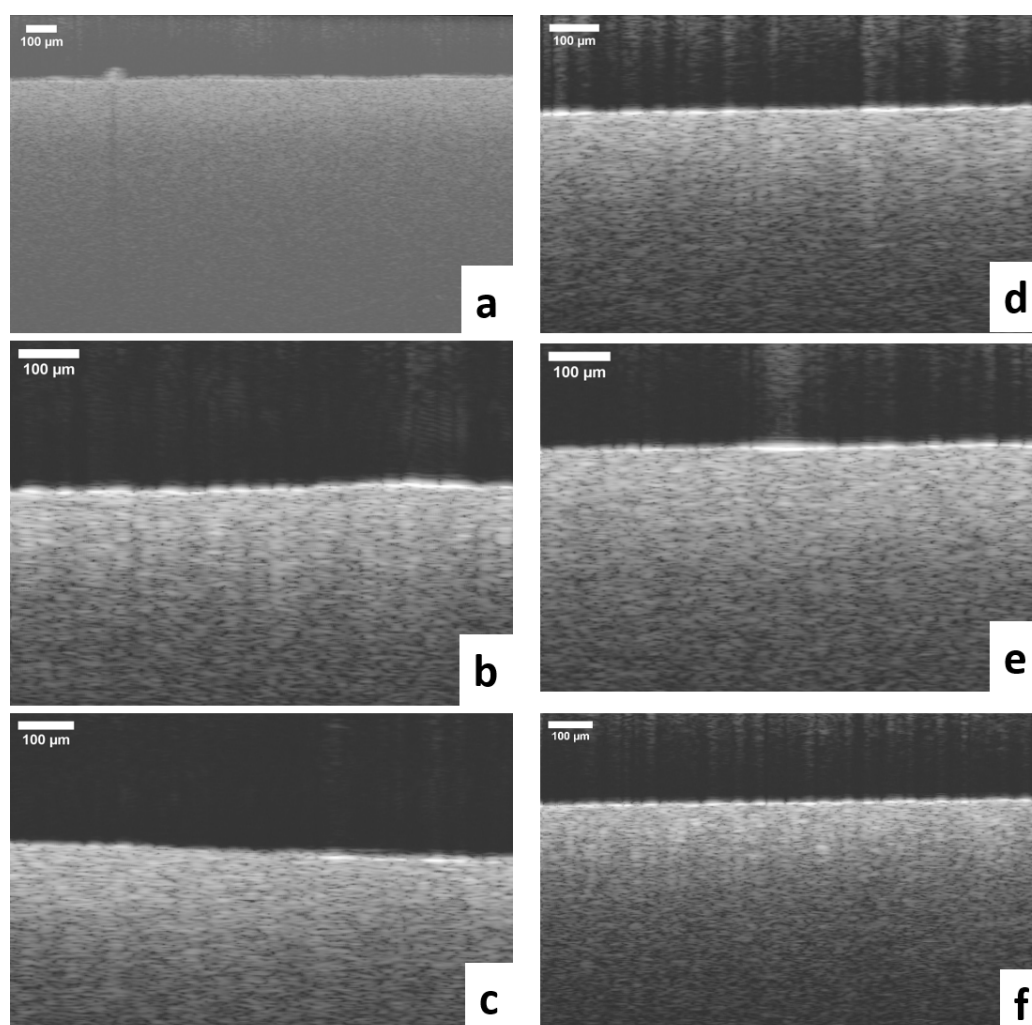


Fig. 4. OCT images of the formation of biofilm: a) Original microsystem and b) Smoothed channel at a flow rate of 0.1 ml/min; c) Original microsystem and d) Smoothed channel at a flow rate of 0.2 ml/min; e) Original microsystem and f) Smoothed channel at a flow rate of 0.3 ml/min

single cells scattered along the channel. In comparison, the untreated microsystem tested at a flow rate of 0.2 ml/min, shows the presence of the extracellular matrix only between the PLA filaments. The *Candida* cells are less packed, with yeast scattered seldomly in the matrix. In the smoothed channel, the colonies

are rare and present only around large pores. The untreated microchannel tested at 0.3 ml/min flow rate showed almost no fungal colonies, with only disjointed extracellular matrix along the PLA filaments. The surface treated channel presented very few sites with extracellular matrix and no *Candida* cells.

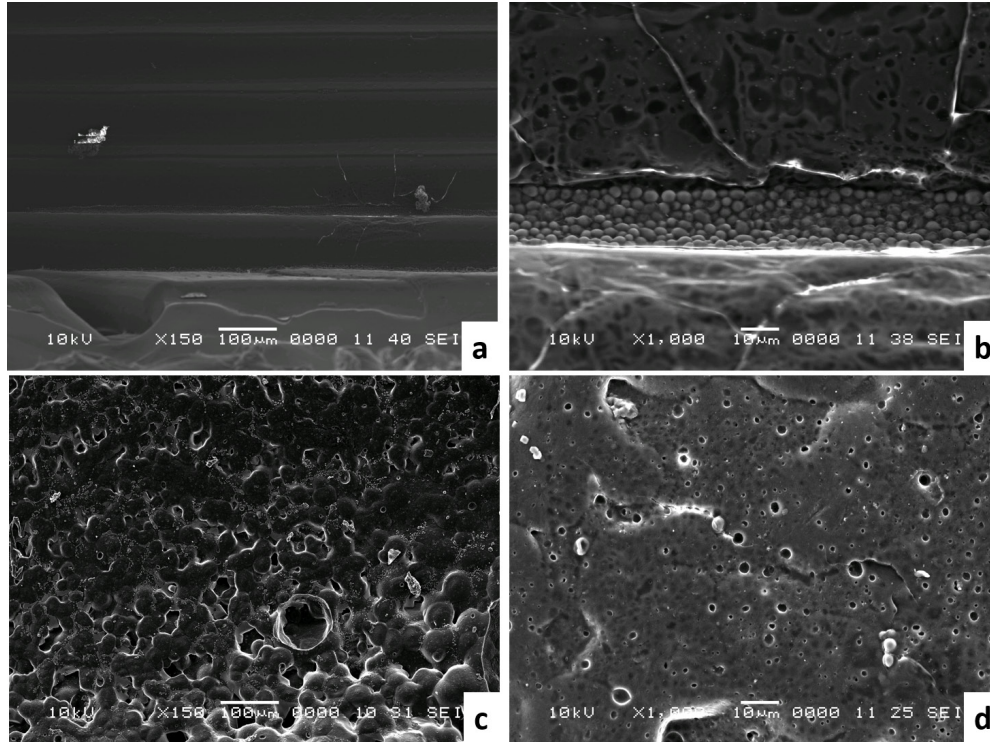


Fig. 5. SEM images of biofilm growth at a flow rate of 0.1 ml/min in an original microsystem at magnifications of a) 150 \times and b) 1000 \times , and in a smoothed channel at magnifications of c) 150 \times and d) 1000 \times

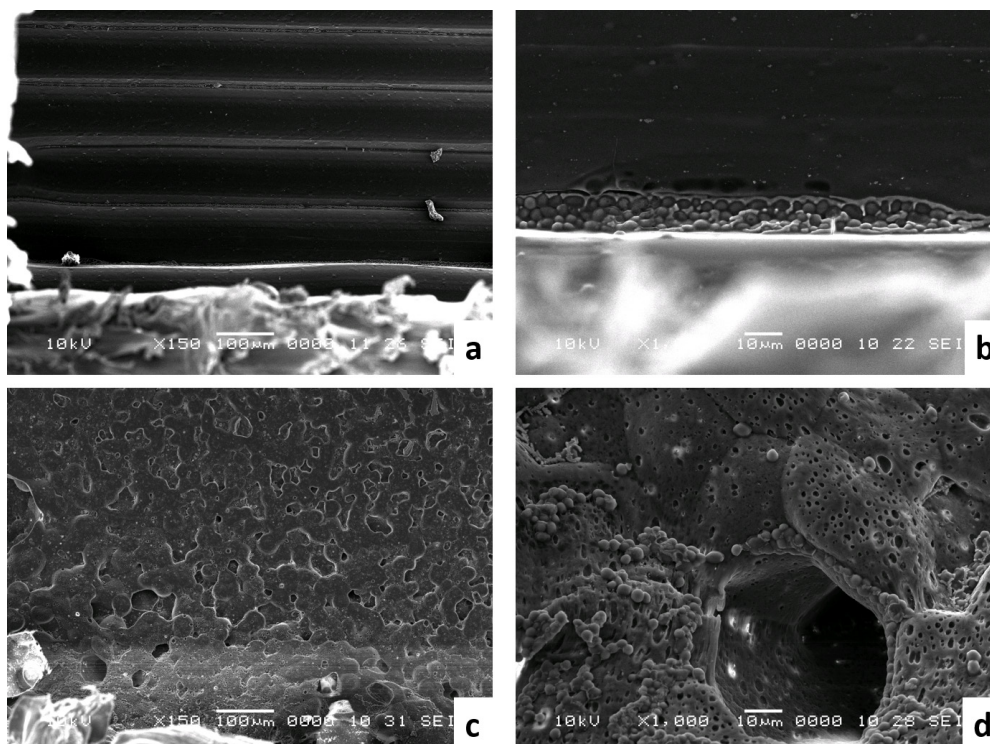


Fig. 6. SEM images of biofilm growth at a flow rate of 0.2 ml/min in an original microsystem at magnifications of a) 150 \times and b) 1000 \times , and in a smoothed channel at magnifications of c) 150 \times and d) 1000 \times

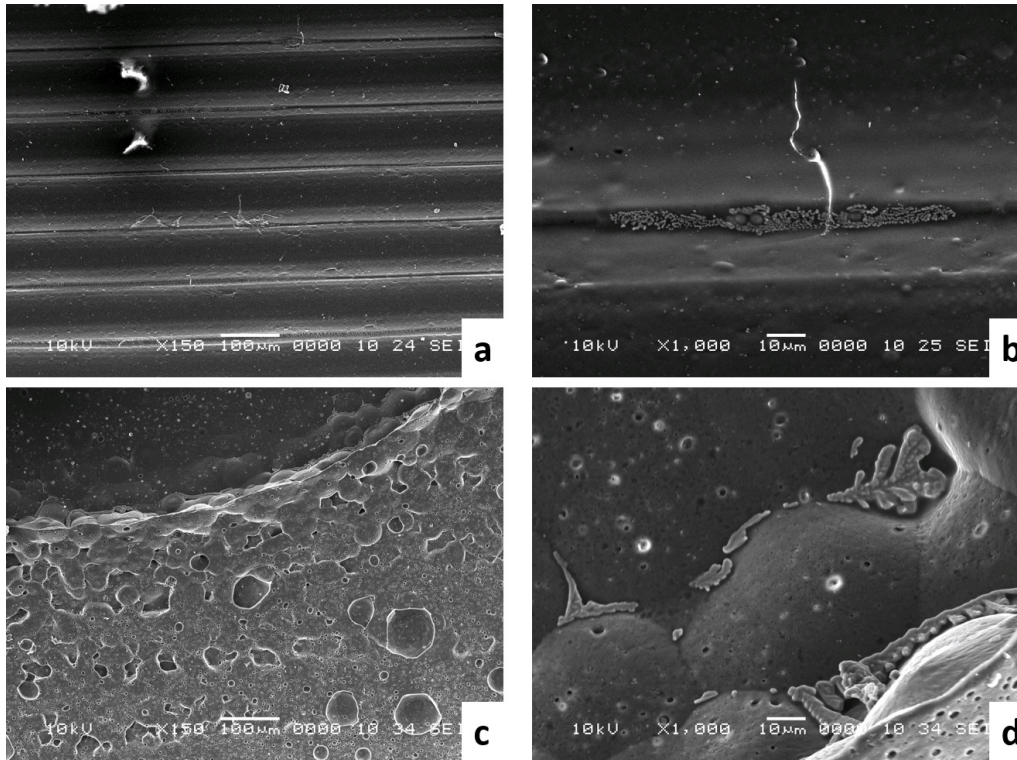


Fig. 7. SEM images of biofilm growth at a flow rate of 0.3 ml/min in an original microsystem at magnifications of a) 150× and b) 1000×, and in a smoothed channel at magnifications of c) 150× and d) 1000×

The quantitative test performed has further strengthened these observations. Using the Beer-Lambert Law, Eq. (1), applied for the absorbance of the ethanol-acetone solutions obtained after the last wash of the microsystems, the concentration of *Candida albicans* biofilm in each microsystem was determined.

$$A = \epsilon \times l \times c \quad (1) [26]$$

where A is the absorbance (nm), ϵ is the molar absorptivity ($M^{-1}cm^{-1}$), l represents the path length of the light (cm), and c is the concentration of the biofilm. The measurements were done by comparison to the known absorbance of the crystal violet, 590 nm, at a path length of 1 cm, and molar absorptivity of $87.00 M^{-1}cm^{-1}$. Table 1 shows the results obtained for each microsystem:

TABLE 1

Concentration of biofilm in both types of microsystems at different flow rates

Type of microsystem	Flow rate (ml/min)	A (nm)	ϵ ($M^{-1}cm^{-1}$)	l (cm)	c (mol/L)
Original	0.1	0.496	87	1	57×10^{-4}
Smoothed	0.1	0.320	87	1	36×10^{-4}
Original	0.2	0.392	87	1	45×10^{-4}
Smoothed	0.2	0.246	87	1	28×10^{-4}
Original	0.3	0.271	87	1	31×10^{-4}
Smoothed	0.3	0.156	87	1	17×10^{-4}

Fig. 8 shows the comparative chart between the decrease in the concentration of biofilm in both smoothed and original

microsystems, versus the flow rate. The difference in concentration is noticeable between the untreated and surface treated microsystems, and the decrease is proportional in both types of microchannels.

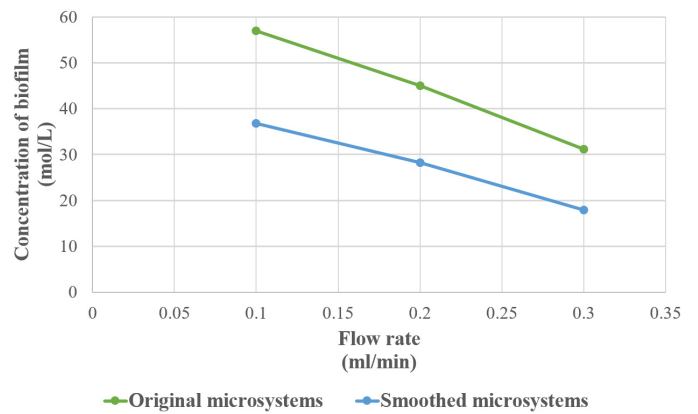


Fig. 8. Comparative chart of the biofilm concentration in original and in-situ surface treated microsystem versus of flow rate

The average dynamic viscosity measured for the prepared fungal solutions with the Brookfield DV2T Viscometer was approximately 1 mPa*s at an average rotation speed of 170 RPM, with no noticeable differences between the tested turbidity values of the *Candida* suspensions. Using Eq. (2) the Reynolds number was determined.

$$Re = \frac{\rho u L}{\mu} \quad (2) [27]$$

where ρ is the density of the fluid (kg/m^3), u is the flow speed (m/s), L is the linear dimension (m) and μ is the dynamic viscosity. To determine the Reynolds number, the flow velocity was calculated using Eq. 3:

$$Q = A \times v \quad (3) \text{ [28]}$$

where Q is the flow rate (ml/min) within the microsystem and A represents the cross-sectional area of the microchannel (mm^2). The small value obtained for the Reynolds number indicates a laminar flow within the central channel of the microsystem.

As it can be observed, the difference in length and height of the PLA droplet in the optical microscopy images for the original and vapor treated microsystems is small, indicating that the vapor treatment, despite producing a local flow of the PLA filaments, did not efficiently smooth the surface channel. However, flushing the system with the organic solvent caused the local dissemination of the PLA, resulting in an almost smooth surface. Moreover, the OCT and SEM images confirm these observations.

The *Candida* suspension was tested at different flow rates in both types of the microfluidic systems to determine the influence of the surface roughness, as well as the influence of the flow velocity on the formation and growth of the biofilm. The SEM images provide a good perspective on the areas where the biofilm has formed and grown within the channels. In the microsystems that had not undergone surface treatment, the biofilm tended to form along the PLA filaments, whereas in the microsystems that had been smoothed through flushing, the biofilm formed and grew in the pores resulted from the in-situ surface treatment. During the SEM investigations, a preferential formation and growth of biofilm was observed. Based on the images obtained, it can be noted that the biofilm has formed on the side of the channel corresponding the side on which the *Candida* suspension was pushed, potentially indicating that the flow within the channel is laminar, with little to no mix between the two fluids.

By comparing the images of the microchannels that have not undergone surface treatment, at different flow rates, it can be observed that the presence of *Candida albicans* colonies decreases with the increase of the flow rate. This can be attributed to the shear stress, which can induce cell detachment and block cell interactions [29]. Similarly, the presence of fungal colonies is highly diminished in the channels that have undergone a surface treatment. This could be explained by the smooth walls of the channels: the absence of rugged surfaces provides little to no attachment surface for the yeast, leading to singular cells scattered along the channel.

4. Conclusions

The proposed manufacturing method using inexpensive materials was found to provide highly reproducible microfluidic devices with the possibility of designing and producing very complex shapes. For a good and predictable functioning of the microfluidic devices when employed for cells suspensions, a surface treatment of the channel was considered. An adequate

smoothing of the PLA microsystems was determined to be through Chloroform flushing. The effect of the smoothing was tested through the growth of a *Candida albicans* (ATCC 10231) biofilm under dynamic conditions.

The OCT images illustrate the formation of a biofilm on the surface of the channels, with a thickness between 4-10 μm . The SEM images indicate that the formation of biofilm is enabled by the existence of rough surfaces (indents of the PLA deposited filaments). In conjunction with the quantitative analysis, it has been observed that less biofilm forms in the smoothed channels, indicating that the behaviour of cells within a flow can be studied more efficiently in the in-situ surface treated microsystems.

Acknowledgments

This work was supported by the grants of the Romanian Ministry of Research and Innovation, CCCDI-UEFISCDI, Project number PN-III-P1-1.2-PCCDI-2017-0221/59 PCCDI/2018 (IMPROVE), within PNCDI III and Project number PN-III-P1-1.2-PCCDI-2017-0010/ 74PCCDI / 2018, within PNCDI III.

REFERENCES

- [1] E.K. Sackmann, A.L. Fulton, D.J. Beebe, *Nature* **507** (7491), 181-189 (2014). DOI: <https://doi.org/10.1038/nature13118>
- [2] J. Cottet, P. Renaud, *Introduction to microfluidics*. Elsevier Inc. (2021).
- [3] C. Chen, B.T. Mehl, A.S. Munshi, A.D. Townsend, D.M. Spence, R.S. Martin, *Anal. Methods* **8** (31), 1-8 (2016). DOI: <https://doi.org/10.1039/C6AY01671E>
- [4] G.S. Fiorini, D.T. Chiu, *Biotechniques* **38** (3), 429-446 (2005). DOI: <https://doi.org/10.2144/05383RV02>
- [5] H. Nabesawa, T. Hitobo, S. Wakabayashi, T. Asaji, T. Abe, M. Seki, *Sensors Actuators, B Chem.* **132** (2), 637-643 (2008). DOI: <https://doi.org/10.1016/j.snb.2008.01.050>
- [6] H. Becker, W. Dietz, *Proc. SPIE 3515, Microfluidic Devices and Systems*, vol. 3515, (1998). DOI: <https://doi.org/10.1117/12.322081>
- [7] Y. Xia, G.M. Whitesides, *Annu. Rev. Mater. Sci.* **28**, 153-184 (1998). DOI:10.1146/annurev.matsci.28.1.153
- [8] T. Schaller, L. Bohn, J. Mayer, K. Schubert, *Precision Engineering* **23** (4), 229-235 (1999). DOI: [https://doi.org/10.1016/S0141-6359\(99\)00011-2](https://doi.org/10.1016/S0141-6359(99)00011-2)
- [9] J. David Beebe, Jeffrey S. Moore, Qing Yu, Robin H. Liu, Mary L. Kraft, Byung-Ho Jo, Chelladurai Devadoss, *Proc. Natl. Acad. Sci. U.S.A.* **97** (25), 13488-13493, (2000). DOI: <https://doi.org/10.1073/pnas.250273097>
- [10] M. Alizadehgiashi, A. Gevorgian, M. Tebbe, M. Seo, E. Prince, E. Kumacheva, *Adv. Mater. Technol* **3** (7), 1-8, (2018). DOI: <https://doi.org/10.1002/admt.201800068>
- [11] M.A. Caminero, J.M. Chacón, I. García-Moreno, G.P. Rodríguez, *Compos. Part B I.* **148**, 93-103 (2018). DOI: <https://doi.org/10.1016/j.compositesb.2018.04.054>

- [12] T.C. Lee, R. Ramlan, N. Shahrubudin, T.C. Lee, R. Ramlan, *Procedia Manuf.* **35**, 1286-1296 (2019). DOI: <https://doi.org/10.1016/j.promfg.2019.06.089>
- [13] G. Gaal, M. Mendes, T.P. de Almeida, M.H.O. Piazzetta, Â.L. Gobbi, A. Riul Jr., V. Rodrigues, *Sensors Actuators, B Chem.* **242**, 35-40 (2017). DOI: <https://doi.org/10.1016/j.snb.2016.10.110>
- [14] D. Pranzo, P. Larizza, D. Filippini, G. Percoco, *Micromachines* **9** (8), 374 (2018). DOI: <https://doi.org/10.3390/mi9080374>
- [15] J.W. Costerton, G.G. Geesey, K.J. Cheng, *Sci. Am.* **238** (1), 86-95 (1978). DOI: <https://doi.org/10.1038/scientificamerican0178-86>
- [16] J.W. Costerton, P.S. Stewart, S Ogden, *Scientific American, Inc.*, 2001.
- [17] N. Vyas, R.L. Sammons, O. Addison, H. Dehghani, A.D. Walmsley, *Nat. Publ. Gr.* **6** (1), 2-11 (2016). DOI: <https://doi.org/10.1038/srep32694>
- [18] J. W. Costerton, *Science* **248** (5418), 1318-1322 (1999). DOI: <https://doi.org/10.1126/science.284.5418.1318>
- [19] J. Azeredo et al., *Critical Reviews in Microbiology* **43** (3), 313-351 (2017). DOI: <https://doi.org/10.1080/1040841X.2016.1208146>
- [20] C. Wilson et al., *Res. Rev. J. Eng. Technol.* **6** (4), (2017). Available online: <https://www.ncbi.nlm.nih.gov/pmc/articles/PMC6133255/> – PMC – PubMed, accessed: 09.04.2021
- [21] J. Hou et al., *Scientific Reports* **9** (1), 1-12 (2019). DOI: <https://doi.org/10.1038/s41598-019-46196-7>
- [22] T.H.B. Singh, J.S. Chohan, R. Kumar, *Materials Today: Proceedings* **26** (3), 3497-3502 (2020). DOI: <https://doi.org/10.1016/j.matpr.2020.04.553>
- [23] J.S. Chohan, R. Singh, K.S. Boparai, R. Penna, F. Fraternali, *Compos. Part B Eng.* **117**, 138-149 (2017). DOI: <https://doi.org/10.1016/j.compositesb.2017.02.045>
- [24] A.J. Rajan, M. Sugavaneswaran, B. Prashanthi, S. Deshmukh, S. Jose, *Mater. Today Proc.* **22** (4), 2772-2778 (2020). DOI: <https://doi.org/10.1016/j.matpr.2020.03.408>
- [25] A. Lalehpour, A. Barari, *IFAC-PapersOnLine* **49** (31), 42-48 (2016). DOI: <https://doi.org/10.1016/j.ifacol.2016.12.159>
- [26] R.W. Ricci, M.A. Ditzler, L.P. Nestor, *J. Chem. Educ.* **71** (11), 983-985 (1994). DOI: <https://doi.org/10.1021/ed071p983>
- [27] V. Slapar, *Microfluidics-Seminar, University of Ljubljana Faculty of Mathematics and Physics Department of Physics*, 19 (2008).
- [28] J.P.Giroud, B. Palmer, J.E. Dove, *Geosynthetics International, Special Issue on Liquid Collection Systems* **7** (4-6), 583-600 (2000). DOI: <https://doi.org/10.1680/gein.7.0183>
- [29] A. Park, H. H. Jeong, J. Lee, K. P. Kim, C.S. Lee, *Biochip J.* **5** (3), 236-241 (2011). DOI: <https://doi.org/10.1007/s13206-011-5307-9>